MAPPING THE SPATIAL DISTRIBUTION OF URBAN HEAT ISLANDS IN DARHAN AND ERDENET CITIES, MONGOLIA

B.Byambadolgor and D.Amarsaikhan
Institute of Geography and Geoecology, Mongolian Academy of Sciences
Email: byambadolgor@mas.ac.mn

KEYWORDS: Urban heat island, Land cover, Normalized Difference Built-up index, Spatial distribution

ABSTRACT: Over the last decades, the phenomenon of urban heat islands (UHI) has been extensively observed in larger cities of the world. This phenomenon is caused by the rapid urbanization and transformation of pastures, forests, croplands, and meadows into waterproof surfaces such as cement, metals, and asphalt. In general, the UHI plays an important role in the study of various interrelated areas, such as urban climate, urban ecology, urban geography, and many other urban related issues.This study examines the changes in the spatial distribution of UHI in the larger cities of Mongolia such as Darkhan and Erdenet, and also investigates the relationship between UHI and the normalized difference built-up index (NDBI) for each land cover class. The NDBI index was useful for detecting impervious surfaces. We have used the Landsat data (TM and OLI) of 2010 and 2020 to observe the land cover changes (vegetation, built-up area, water, and bare land) in the selected cities. For the derivation of the land cover classes an object-based image classification was applied. Also, we used the Local Moran's I statistical method to detect the spatial distribution of UHIs. Emphasizing the important role of green space in mitigating the impact of UHI, it is recommended that green space should be considered in landscape and urban planning.

1. INTRODUCTION

At present, the continuous flow of migration from rural areas to towns and cities around the world is rapidly expanding the boundaries of cities. According to the United Nations study from 2016 to 2030, population over centralization in urban areas has been observed, and this centralization will take place in 64% of all developing countries and 86% of developed countries by 2050 (United Nations, 2018).

In Mongolia, the flow of the population towards urban areas has continued, and since 1998 this flow has increased and as of 2020, 69% of the total population lives in urban areas, of which 47.6% or almost one in two persons live in the capital city (National Statistic Information Service, 2022). In addition to Ulaanbaatar, in the major provincial capitals such as Erdenet and Darkhan, the number of people migrating from the rural areas have been continuously increased in recent years. Also, due to the rapid urbanization in these cities, the city's boundaries and ger areas have expanded without control, and have had a significant impact on the use of natural resources and the environment.

With rapid urbanization, areas such as crops, pastures, forests, and meadows are mostly transformed into impervious surfaces such as cement, metal, and asphalt. It has many negative effects, such as degrading the environment, increasing environmental pollution, increasing the air temperature, and reducing the urban greenspace (Min et al. 2011). Consequently, as a result of urbanization, the UHI phenomenon, which is a major microclimatic phenomenon of the city, is intensively observed.

The UHI phenomenon refers to the fact that the air and land surface temperature (LST) of a city or settlement become warmer than the local temperature of the place. This phenomenon is due to significant changes in land cover and land use (LULC) and urban landscape due to rapid urbanization. In other words, the UHI phenomenon is affected by the reduction of vegetation, the characteristics of building materials, geometry, and density, anthropogenic heat, weather, and geographical location (Hua, et al. 2010; Bhatta, 2010). The phenomenon of UHI creates many negative environmental effects such as air pollution, increase in greenhouse gas emissions, impact on human health, loss of water resource use, and biodiversity habitat (Xiao et al. 2018). Thus, the phenomenon of the UHI occupies an important place in the study of various interrelated fields such as urban climate, urban ecology, and urban planning.

In recent years, remote sensing (RS) data, combined with spatial analysis methods, have been widely used to study the spatial distribution of UHIs, the relationship between LULC and urban landscape patterns and LST, and the dynamic change of urban climate and its impact on the environment. For example, García-Cueto et al. (2007) used the data of air temperature and surface temperature retrieving from both NOAA's AVHRR and Landsat thermal images to study the relationship between UHI and LULC at different spatial and temporal resolutions (Zhang et al. 2013; García-Cueto et al. 2007). Estoque et al. (2017) finds a significantly strong correlation between the mean LST and the density of Normalized Difference Built-up Index (NDBI) (positive), green space (negative), and the size,

shape complexity, and aggregation of patches along the urban-rural gradients of several cities. Berger et al. (2017) showed that the positive correlation between LST and NDBI shows that the UHI effect is increasing in developed countries, and that green building are highly effective in reducing the UHI. In developed and developing countries of the world, research on the relationship between LULC and LST is prioritized, but in Mongolia, this type of research is insufficient.

2. RESEARCH MATERIALS AND METHODOLOGY

2.1 Study area

Darkhan and Erdenet cities have been selected as study areas. The cities play a major role in infrastructure, public services, education, commerce, agriculture, industrialization and the regional economy. As of 2020, Darkhan City has a population of 85,887 and Erdenet City has a population of 103,735, and the migration of the population from rural areas to these areas has been intensive in recent years. In terms of geographical location, the city of Darkhan belongs to the Orkhon-Selenge basin, the bank of the Kharaa river located in the Burhant valley, and it is located at an altitude of 700 m above sea level. The city of Erdenet is located in the Orkhon and Selenge basins, in the lap of the Bureng mountain range, a branch of the Khangai mountain range, at 1300 m above sea level.

2.2 Data resources and pre-processing

The Landsat images used in this study have been downloaded from the U.S. Geological Survey site, and two Landsat TM images (23 August 2010 and 30 August 2010), and two Landsat OLI image (18 August 2020 and 10 September 2020) were obtained. The Landsat TM and Landsat OLI data have been geometrically and radiometically corrected to remove positional errors and atmospheric inferences. All image bands 1–5 and 7 have a spatial resolution of 30 m, and the thermal infrared band has a spatial resolution of 120m for Landsat TM and 100m for Landsat-8 OLI image.

2.3 LULC classification

In the current study, we used an object-based image analysis method to classify the study area into four land cover categories, namely built-up area, vegetation (such as forest, shrubs, and grass), bare soil, and water. OBIA is one of the most popular classification methods for using spectral, geometric, contextual, and textural information of image objects, which gives better results in the classification process (Dingle Robertson, 2011). For the classification, eCognition Developer was utilized.

2.4 Land surface temperature retrieval

Before calculating the LST of the cities, the Normalized difference vegetation index (NDVI) was calculated using the following formula.

$$NDVI = \frac{(NIR-Red)}{(\mathrm{NIR+Red})} \quad (1)$$

The standard method for retrieving LST from raw Landsat datasets requires the conversion of the digital number (DN) values of the thermal bands (band 6 in Landsat TM and Bands 10) first into absolute radiance values. These radiance values are then used to derive at satellite brightness temperature, calculated under an assumption of unity emissivity and using pre-launch calibration constants (Estoque et al. 2017). This process is followed by a correction for spectral emissivity according to the nature of the landscape. In this study, we used the preprocessed Band 10 of Landsat-OLI, containing top of atmosphere brightness temperature values expressed in Kelvin to produce an LST map for each of the study areas. After converting the brightness temperature values into degrees Celsius (°C), the emissivity-corrected LST was calculated as follows.

$$L\lambda = \frac{(\mathrm{Lmax}\lambda-\mathrm{Lmin}\lambda)}{(\mathrm{Qcalmax}-\mathrm{Qcalmin})} \times (\mathrm{Qcal}-\mathrm{Qcalmin}) + \mathrm{Lmin}\lambda \quad (2)$$

where $L\lambda$ is at-sensor spectral radiance ($W*m^{-2}\ sr^{-1}\ \mu\ m^{-1}$); Lmin is the TOA radiances for band 6 (Landsat TM) and band 10 (Landsat OLI) at DNs; QCALmax = 255 and QCALmin = 0 are the maximum and minimum quantized calibrated values, respectively; and Lmax and Lmin are the spectral radiance scaled to QCALmax and QCALmin ($W*m^{-2}\ sr^{-1}\ \mu\ m^{-1}$), respectively.

To retrieve the LST values, we firstly derived the land surface emissivity (ε) values Equation.3:

$$\varepsilon = \mathrm{mPV} + \mathrm{n} \quad (3)$$

Where m= ($\varepsilon - \varepsilon$) − (1 − $\varepsilon\ \sigma$) Fε v and n = ε s + (1 − ε s) Fε v, where ε s and ε v are the soil emissivity and vegetation emissivity, respectively. We used the result of form= 0.004 and n = 0.986. PV is the proportion of vegetation extracted from the NDVI Equation.4:

$$PV = \left(\frac{NDVI - NDVImin}{NDVImax - NDVImin}\right)^2 \quad (4)$$

Conversion of spectral radiance to temperature in Celsius Equation.5:

$$T = \frac{K2}{\mathrm{Ln}\left(\frac{K1}{L\lambda}+1\right)} - 273.15 \quad (5)$$

where; T is brightness temperature in Celsius, K1 and K2 are thermal conversion constant for the band. For Landsat TM, K1 = 607.76 W/ (m^2* sr * µm) and K2 =1260.56; for Landsat OLI, K1 = 774.89 ($W*m^{-2}$ sr^{-1} µ m^{-1}); and K2 =1321.08 Kelvin.

The NDBI is an index for identifying and classifying built-up areas or impervious surfaces. The NDBI is expressed as Equation.6:

$$NDBI = \frac{(SWIR - NIR)}{(SWIR + NIR)} \quad (6)$$

where MIR = band 5 (for Landsat TM—wavelength 1.55–1.75 µm) and band 6 (for Landsat 8—wavelength 1.57–1.65 µm) and NIR = band 4 (for Landsat TM—wavelength 0.76–0.90 µm) and band 5 (for Landsat OLI—wavelength 0.85–0.88 µm).

2.5 Spatial autocorrelation analysis

The relationship between LST, NDVI, and NDBI was analyzed by linear regression for each LULC class using SPSS software. Also, their spatial distribution was determined using Moran's index (I), one of the measures of spatial autocorrelation. Global Moran's I tool spatially assesses patterns in a data set and determines whether it is distributed, clustered, or random based on the location and value of a feature. The tool calculates Moran's I index value along with z-score and p-value and validates the index statistically (Getis, 2010).

$$I = \frac{n}{S_o} \frac{\Sigma_{i=1}^{n} \Sigma_{j=1}^{n} w_{i,j} z_i z_j}{\Sigma_{i=1}^{n} z_i^2} \quad (7)$$

Where z_i stands for deviation of an attribute from its mean ($x_i - X\square$) for feature X, $w_{i,j}$ is the spatial weight among feature i and j, n is equal to the total number of features, and S_o is the aggregate of all the spatial weights.

$$S_o = \Sigma_{i=1}^{n} \Sigma_{j=1}^{n} w_{i,j} \quad (8)$$

The z_i-score for the statistics is computed as: $Zi = \frac{I - E[I]}{\sqrt{V[I]}}$

$$\text{where: } E[I] = -1/(n-1); \qquad V = E[I^2] - E[I^2] \quad (9)$$

The cluster map generates four clusters: High-high, low-high, low-low, and high-low, where high-high indicates variables with high values surrounded by high values, low-high indicates variables with low values surrounded by low values, and likewise for low-low and high-low. Finally, the significance map shows at which statistical levels there are significant correlations.

3. RESULTS AND DISCUSSION

3.1 Spatio-temporal analysis of LULC

The land cover of Darkhan and Erdenet cities was classified using the object-based classification method. The overall classification accuracy was 83.01% in Darkhan and 80.37% in Erdenet in 2010, and 85.27% in Darkhan and 83.9% in Erdenet in 2020. As seen from LULC study of Darkhan city, the built-up area was increased by 4.77%, the vegetation area by 1.7%, and water by 0.18%, while bare soil was decreased by 6.65%. The built-up area in Darkhan was increased from 4.1% to 6.1% of total area during the period of 2010–2020. Table 1 indicated that vegetation decreased by− 3.1%, water decreased by -0.6%, and bare soil increased by 1.7% during the study period.

Table 1. Area for each of the LULC classes during the years 2010 and 2020.

Cities	**Darkhan**		**Erdenet**	
	Area /$km^{2/}$			
LULC	2010	2020	2010	2020
Vegetation	57.69	59.48	162.36	153.76
Bare-soil	28.1	21.6	96.23	100.94
Built-up area	10.43	14.98	11.3	16.83

Water	1.29	1.45	6.63	4.99

3.2 Spatio-temporal analysis of LST

The spatial distribution of LST in Darkhan and Erdenet cities is given in Figure 1. The mean LST for built-up areas was expanded from 23°C to 28.2°C during the 2010-2020 period. Similarly, LST for bare soil ranged from 23°C to 28.16°C. The highest LST value was 34.1°C in Erdenet city and 30.9°C in Darkhan city in 2010, while their values in 2020 were 32.6°C and 28.3°C. The lowest temperature of the cities was observed in Erdenet (14.7°C). Results indicated that in Darkhan city in 2010, the LST above 30 degrees accounted for 5.6% of the total area, while the LST between 25-29 degrees accounted for 81.3%. Also, in Erdenet city in 2010, the LST above 30 degrees accounted for 20.84% of the total area, while the LST between 25-29 degrees accounted for 60.63%.

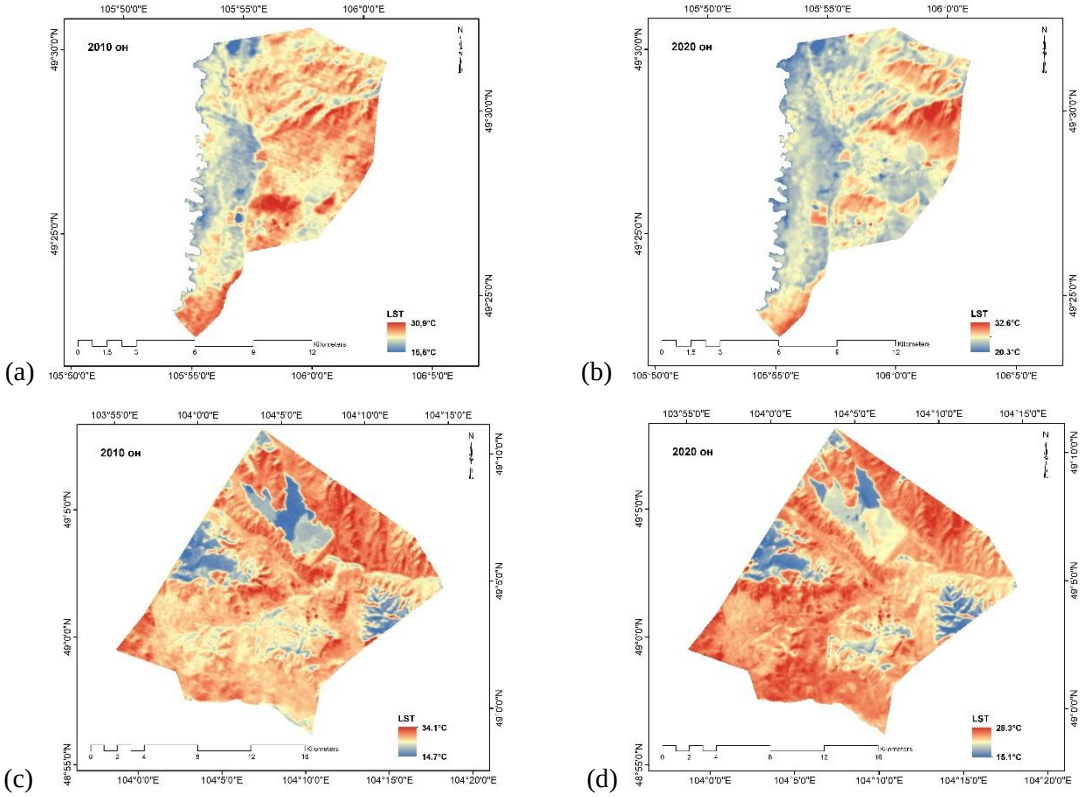

Figure 1. Spatial distribution of LST in Darkhan (a, b) and Erdenet (c, d) cities.

The NDBI values of the cities ranged from -0.368 to 0.474 in Darkhan and from -0.737 to 0.375 in Erdenet, and their average values were 0.009 and 0.203 in 2010. In 2020, the NDBI values of cities ranged from -0.453 to 0.241 in Darkhan and from -0.302 to 0.374 in Erdenet. On the other hand, the average values of NDBI of cities were 0.227 and 0.256 in 2020 and it is observed that the average value of NDBI of cities has increased over 10 years.

3.3. Correlation between LST and NDVI NDBI

The relationship between LST, NDVI and NDBI is discussed for each LULC class. The results showed a negative correlation between LST and NDVI and a positive correlation between LST and NDBI (Chen, 2006; Laosuwan, 2012; Bakar, et al., 2016). This observation is very consistent with the results of several studies in this direction. The negative NDVI coefficient and positive NDBI coefficient for the two dates in Darkhan and Erdenet cities indicate that within the study area, vegetation contributes to reducing the UHI effect, while the residential area increased the UHI effect. There was a weak negative correlation between LST and NDVI in the 2010 vegetation class of cities, and this correlation decreased in 2020. There was a weak negative correlation between LST and NDVI in the class with built-up area in Darkhan city in 2010, but it changed to a weak positive correlation in 2020. Considering the relationship between LST and NDBI of cities, a weak positive relationship was observed in Darkhan city and a strong positive relationship was observed in Erdenet city. But for other classes, it can be observed that their correlation was weakly positive (Table 2, 3). This relationship shows that in the process of intensive urbanization, the urban population has increased significantly, the built-up area and the boundaries of residential areas have expanded uncontrollably, and the impervious surface area has increased significantly.

Table 2.Relationship between LST and NDVI in cities.

	Darkhan city			
	2010		2020	
LULC	Equations	R^2	Equations	R^2
Vegetation	LST= -9.68 x NDVI + 27.45	0.359	LST= - 16.09 x NDVI + 31.13	0.189
Bare-soil	LST= -6.44 x NDVI + 27.58	0.032	LST= 10.81 x NDVI + 20.69	0.439
Built-up area	LST= -3.52 x NDVI + 26.22	0.091	LST= 5.57 x NDVI + 27.16	0.085
Water	LST= 3.73 x NDVI + 22.27	0.044	LST= 3.25 x NDVI + 22.72	0.077
	Erdenet city			
	2010		2020	
LULC	Equations	R^2	Equations	R^2
Vegetation	LST= - 20.07 x NDVI + 33.11	0.387	LST= - 2.37 x NDVI + 23.08	0.002
Bare-soil	LST= 12.88 x NDVI + 23.94	0.429	LST= 10.9x NDVI + 22.25	0.088
Built-up area	LST= 0.97x NDVI + 25.78	0.003	LST= 3.44 x NDVI + 22	0.035
Water	LST= 4.58 x NDVI + 17.83	0.128	LST= 9.53 x NDVI + 17.77	0.217

Table 3. Relationship between LST and NDBI in cities

	Darkhan city			
	2010		2020	
LULC	Equations	R^2	Equations	R^2
Vegetation	LST= 9.16x NDBI + 22.91	0.325	LST= 22.08 x NDBI + 28.06	0.400
Bare-soil	LST= 8.78 x NDBI + 24.3	0.086	LST= 21.26x NDBI + 27.77	0.294
Built-up area	LST= 9.19 x NDBI + 26.54	0.112	LST= 6.41 x NDBI + 24.51	0.150
Water	LST= 17.26 x NDBI + 21.44	0.135	LST= 1.66x NDBI + 23.46	0.003
	Erdenet city			
	2010		2020	
LULC	Equations	R^2	Equations	R^2
Vegetation	LST= 25.14 x NDBI + 20.8	0.675	LST= 34 x NDBI + 23.23	0.663
Bare-soil	LST= 15.75 x NDBI + 21.98	0.171	LST= 10.9 x NDBI + 22.25	0.088
Built-up area	LST= 3.55 x NDBI + 22.57	0.011	LST= 10.81 x NDBI + 26.68	0.090
Water	LST= 3.98 x NDBI + 17.26	0.135	LST= -7.45 x NDBI + 16.94	0.010

Moran's I statistics has been widely applied in hotspot identification in research areas such as infrastructure planning and management (Carroll, 2008), tourism management (Yang, 2013), health and environmental impact assessment (Browning, 2018), and UHI assessment (Majumdar, 2016). In the study, we used the local Moran's I method to map the spatial distribution of vulnerable and sensitive areas to the UHI phenomenon. By applying that statistics, hotspot maps of the Darkhan and Erdenet inner cities were created on two different dates (Figure 2). This will provide a better understanding of urban UHI effects. The maps show that hotspots are highly clustered in the bare soil. The cold cluster correspond to areas with extensive vegetation and rivers. Hotspot cluster tends to expand over time. It is seen that when LST increases, some cold cluster areas tend to become hotspots. HH cluster or high LST values occupied 5.7% and 12.6% of the total area of Darkhan and Erdenet cities, while LL clusters or areas with low LST values occupied 27.6% and 6.2%, respectively. The HH-HH cluster of areas predisposition to UHI phenomenon in Darkhan city accounted for 12.5% of the total area, HH-LL and LL-HH clusters accounted for 0.2%, and LL-LL-13.2%, respectively. However the HH-HH cluster of Erdenet city occupied 4.8% of the total area, LL- HH -0.02%, and LL-LL-7.9%, respectively.

4. CONCLUSIONS

In this study, the relationship between NDVI, NDBI, and LST of Darkhan and Erdenet cities was determined for each LULC class using multitemporal Landsat. According to the study, the phenomenon of UHI was observed in the classes of bare land and built-up areas of the cities. During all periods of the study, the lowest temperatures were observed in the classes of vegetation and water. This shows how green space can reduce the phenomenon of UHI in the city. The linear regression analysis showed a strong positive correlation between LST and NDBI and a weak positive correlation between LST and NDVI, and these correlations tended to increase from year to year. This correlation shows that forests and shrubs around urban areas are deteriorating. When studying the relationship

between LST and NDVI and NDBI in Darkhan and Erdenet cities for different LULC types, the relationship was not linear in some classes and may vary between different LULC types depending on geographical location and other factors. According to the analysis, with the rapid urbanization, the UHI phenomenon in the city will intensify and the areas prone to this phenomenon will increase, so it is very important to plan new green spaces and protect existing green spaces in future urban planning.

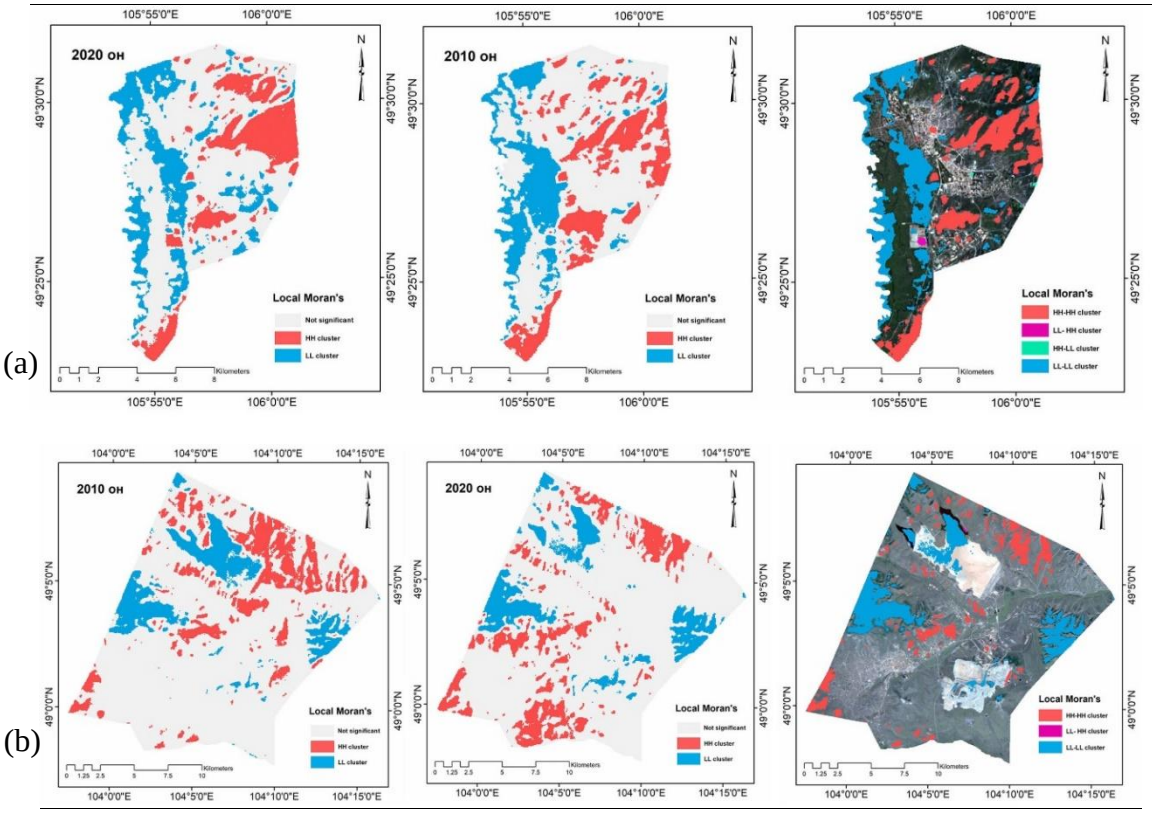

Figure 2. LISA cluster map of the cities (a) Darkhan and (b) Erdenet.

REFERENCES

Bakar, S. B. A., Pradhan, B., Lay, U. S., & Abdullahi, S., 2016. Spatial assessment of land surface temperature and land use/land cover in Langkawi Island. In *IOP Conference Series: Earth and Environmental Science* (Vol. 37, No. 1, p. 012064). IOP Publishing.

Berger, C., Rosentreter, J., Voltersen, M., Baumgart, C., Schmullius, C., & Hese, S., 2017. Spatio-temporal analysis of the relationship between 2D/3D urban site characteristics and land surface temperature. *Remote sensing of environment*, *193*, 225-243.

Bhatta, B., 2010. Causes and consequences of urban growth and sprawl. In *Analysis of urban growth and sprawl from remote sensing data* (pp. 17-36). Springer, Berlin, Heidelberg.

Browning, M. H., & Rigolon, A., 2018. Do income, race and ethnicity, and sprawl influence the greenspace-human health link in city-level analyses? Findings from 496 cities in the United States. *International journal of environmental research and public health*, *15*(7), 1541.

Carroll, M. C., Reid, N., & Smith, B. W., 2008. Location quotients versus spatial autocorrelation in identifying potential cluster regions. *The Annals of Regional Science*, *42*(2), 449-463.

Chen, X. L., Zhao, H. M., Li, P. X., & Yin, Z. Y., 2006. Remote sensing image-based analysis of the relationship between urban heat island and land use/cover changes. *Remote sensing of environment*, *104*(2), 133-146.

Dingle Robertson, L., & King, D. J., 2011. Comparison of pixel-and object-based classification in land cover change mapping. *International Journal of Remote Sensing*, *32*(6), 1505-1529.

Estoque, R. C., Murayama, Y., & Myint, S. W., 2017. Effects of landscape composition and pattern on land surface temperature: An urban heat island study in the megacities of Southeast Asia. *Science of the Total Environment*, *577*, 349-359.

García-Cueto, O. R., JÁUREGUI-OSTOS, E., Toudert, D., & Tejeda-Martinez, A., 2007. Detection of the urban heat island in Mexicali, BC, México and its relationship with land use. *Atmósfera*, *20*(2), 111-131.

Getis, A., & Ord, J. K., 2010. The analysis of spatial association by use of distance statistics. In *Perspectives on spatial data analysis* (pp. 127-145). Springer, Berlin, Heidelberg.

Hua, L., Li, X., Tang, L., Yin, K., & Zhao, Y., 2010. Spatio-temporal dynamic analysis of an island city landscape: a case study of Xiamen Island, China. *International Journal of Sustainable Development & World Ecology*, *17*(4), 273-278.

Laosuwan, T., & Sangpradit, S., 2012. Urban heat island monitoring and analysis by using integration of satellite data and knowledge based method. *International Journal of Development and Sustainability*, *1*(2), 99-110.

Majumdar, D. D., & Biswas, A., 2016. Quantifying land surface temperature change from LISA clusters: An alternative approach to identifying urban land use transformation. *Landscape and Urban Planning*, *153*, 51-65.

Min, L., Fangying, G., Jiawei, F., Meixuan, S., & He, Z., 2011. The sustainable approach to the green space layout in highdensity urban environment: a case study of Macau peninsula. *Procedia Engineering*, *21*, 922-928.

National Statistic Information Service, 2022. https://www.1212.mn/

United Nations, 2018. Revision of World Urbanization Prospects; United Nations Department of Economic and Social Affairs; United Nations: New York, NY, USA.

Xiao, X. D., Dong, L., Yan, H., Yang, N., & Xiong, Y., 2018. The influence of the spatial characteristics of urban green space on the urban heat island effect in Suzhou Industrial Park. *Sustainable Cities and Society*, *40*, 428-439.

Yang, Y., & Wong, K.K., 2013. Spatial distribution of tourist flows to China's cities. *Tourism Geographies*, *15*(2), 338-363.

Zhang, H., Qi, Z. F., Ye, X. Y., Cai, Y. B., Ma, W. C., & Chen, M. N., 2013. Analysis of land use/land cover change, population shift, and their effects on spatiotemporal patterns of urban heat islands in metropolitan Shanghai, China. *Applied Geography*, *44*, 121-133.